Received: 23 March 2023 | Revised: 2 August 2023 | Accepted: 17 August 2023

DOI: 10.1002/pat.6184

RESEARCH ARTICLE

polymers advanced technologies WILEY

Poly(vinylidene fluoride) and thermoplastic polyurethane composites filled with carbon black-polypyrrole for electromagnetic shielding applications

Mayara C. Bertolini[1,2] | Silvia D. A. S. Ramoa[2] | Elaine C. L. Pereira[3] | Bluma G. Soares[3] | Guilherme M. O. Barra[2] | Alessandro Pegoretti[1,4]

[1]Department of Industrial Engineering, University of Trento, Trento, Italy

[2]Department of Mechanical Engineering, Universidade Federal de Santa Catarina, Florianópolis, Brazil

[3]Department of Metallurgical and Material Engineering, Universidade Federal do Rio de Janeiro, Rio de Janeiro, Brazil

[4]National Interuniversity Consortium of Materials Science and Technology (INSTM), Florence, Italy

Correspondence
Mayara C. Bertolini and Alessandro Pegoretti, Department of Industrial Engineering, University of Trento, Trento, Italy.
Email: mayaracbertolini@gmail.com and Alessandro.Pegoretti@unitn.it

Funding information
CAPES - PRINT, Grant/Award Number: 88881.310728/2018-01; CNPq (Conselho Nacional de Desenvolvimento Científico e Tecnológico), Grant/Award Number: 309125/2020-0; Italian Ministry for University and Research (MUR), Grant/Award Number: L.232/2016

Abstract

This study aims to investigate the electromagnetic interference shielding properties of composites based on immiscible polymer blends of poly(vinylidene fluoride) (PVDF) and thermoplastic polyurethane (TPU) filled with carbon black doped with polypyrrole (CB-PPy) prepared by compression molding and fused filament fabrication. Composites of PVDF/CB-PPy and TPU/CB-PPy were also prepared for comparison. Rheological measurements showed that although the rheological behavior of PVDF/TPU composites was an intermediate behavior between PVDF/CB-PPy and TPU/CB-PPy composites, the effect of the conductive filler was much more pronounced in PVDF than in TPU. Moreover, the addition of CB-PPy was found to increase the storage modulus of the composites leading to more rigid materials, and to decrease the T_g values of the composites due to the reduction of the mobility of the polymeric chains. In addition, PVDF/TPU composites presented an intermediate behavior when compared to composites based on the neat polymers demonstrating that the addition of TPU to PVDF contributes to the development of composites with improved flexibility. Furthermore, the addition of CB-PPy increased the electrical conductivity of all composites. However, the electrical conductivity of PVDF/TPU 50/50 vol% co-continuous blends was higher than the electrical conductivity of PVDF/TPU 38/62 vol% composites with the same amount of conductive filler. Composites with higher electrical conductivity showed better shielding from electromagnetic radiation. As expected, composites based on the co-continuous blend displayed higher EMI shielding efficiency than the 38/62 vol% composites. The main mechanism of shielding was absorption for all composites. Overall, composites based on the PVDF/TPU 50/50 vol% co-continuous blend showed a better combination of EMI

shielding efficiency and mechanical properties. Moreover, specimens prepared by fused filament fabrication displayed diminished electrical conductivity and EMI-SE responses when compared to compression-molded samples with the same composition. This difference is attributed to the presence of voids, defects, and overlapping layers, which can hamper the electron flow.

KEYWORDS

carbon filler, conductive composites, electromagnetic interference shielding, fused filament fabrication, polymer blend

1 | INTRODUCTION

The current number of electronic devices, such as mobile phones, wearable smart devices, portable computers, sensors, radars, electrodes, and transmitters, is increasing in areas such as wireless communication, household, aerospace industry, medical and military fields. This technological growth contributes to the enhancement of electromagnetic interference (EMI), which is related to the radiated and conducted electromagnetic signals that can disturb the operation of electronic devices and cause radiative damage to living species. For this reason, numerous studies have reported the development of EMI shielding materials capable of attenuating and dissipating the radiation.[1–10] The electromagnetic shielding effectiveness (EMI-SE) is the ability of the material in attenuating the electromagnetic waves, which is expressed in decibels (dB).

EMI shielding materials can work based on three different mechanisms in a specific frequency range: reflection (R), absorption (A), and multiple reflection (MR). The multiple reflection mechanism represents the internal reflection within the shielding materials and it is commonly insignificant for frequencies in the GHz range.[8,10–13] The shielding effectiveness by reflection (SE_R) is related to the interaction of the electromagnetic radiation with mobile charges carriers, electrons, or holes, however, reflection is a source of secondary pollution because the radiation is reflected in the environment making EMI absorptive materials more attractive.[1,2,9,12,14,15] The shielding effectiveness by absorption (SE_A) is generally associated with electrical and magnetic dipoles that interact with the electromagnetic waves converting the electromagnetic energy into heat.[9,11,12]

Traditional shielding materials are based on metallic sheets due to their high magnetic permeability, high electrical conductivity, and high number of free electron charge carriers that leads to very effective EMI shielding properties.[2,15] However, their shielding mechanism is based on the reflection of the electromagnetic radiation and they generally suffer from poor mechanical flexibility, high weight and density, electrochemical corrosion, and expensive processing techniques.[1,2,6,8,16,17] On the other hand, intrinsically conducting polymers (ICPs) and electrically conductive polymer composites (ECPCs) are getting much attention as EMI shielding materials due to their shielding mechanism mainly based on the absorption of the electromagnetic radiation and its dissipation in the conductive filler particles, which is interesting for numerous applications.[2,8,12,15,17,18] ECPCs offer also the advantages of light weight, ease of processing, corrosion resistance, and low cost.[2–6,8,13,17,19] ECPCs containing intrinsically conducting polymers, carbonaceous fillers, such as carbon nanotubes, carbon black, graphene, and carbon fibers, have been widely studied as EMI shielding materials.[1,6,8,9,18,20]

In this context, many investigations have been carried out aiming at reducing the electrical percolation threshold of ECPCs in order to achieve high electrical conductivity values with the lowest content of conductive filler, thus preserving the mechanical properties and processability of the polymeric matrix.[16,21] Among the various adopted strategies, the preparation of ECPCs based on polymeric matrices composed of immiscible polymer blends in order to selectively localize the conductive filler in one of the polymer phases or at the interface of the polymeric blend is an investigated approach to reduce the percolation threshold of ECPCs.[12,22–32] Furthermore, polymeric blends with a co-continuous phase structure have been reported to manifest a reduced electrical percolation threshold due to a more efficient double percolation phenomenon because of the selective localization of the conductive filler in one phase or at the interface of the polymeric blend.[12,31,32]

Electrically conductive polymer composites for EMI shielding applications are generally fabricated via conventional processing routes such as solvent casting or melt mixing followed by compression molding. Melt compounding is a useful manufacturing method for ECPCs because of its extensive availability in polymer industries and its simplicity.[7] However, a manufacturing technique for large-scale production with freedom in design for parts with complex geometries is still a challenge. In this framework, although the availability of fused filament fabrication (FFF) techniques is getting much attention for the fabrication of ECPCs for EMI shielding applications, several challenges have still to be solved.[1,3–6,15,19,20] The EMI shielding effectiveness depends on several factors including the electrical conductivity of the filler, dielectric constant, and aspect ratio.[14] However, the effect of carbonaceous fillers on electrical and EMI shielding properties of immiscible polymer blends are not very explored, especially when processed by FFF.

In this context, this study proposes the investigation of the electromagnetic shielding properties of composites based on immiscible polymeric blends of poly(vinylidene fluoride) and thermoplastic polyurethane filled with carbon black-polypyrrole as conductive filler and prepared by compression molding and fused filament fabrication. The

morphology of the composites was already discussed in our previous work[33] where a co-continuous structure was observed for one of the blend compositions. For comparison, composites based on the neat polymers PVDF/CB-PPy and TPU/CB-PPy are also investigated in this study.

2 | EXPERIMENTAL

2.1 | Materials

Amboflon® PVDF 24 with a relative density of 1.78 g.cm^{-3}, a melt flow index of 22 g.10 min^{-1}, a melting temperature of 165–175°C and an electrical conductivity of 10^{-13} S.cm^{-1} was purchased from Ambofluor GmbH & Co. TPU Desmopan® DP 6064 is an ether-based polyurethane provided by Covestro AG with a relative density of 1.09 g.cm^{-3}, an injection molding temperature of 200–220°C and an electrical conductivity of 10^{-11} S.cm^{-1}. The conductive filler used in this study is carbon black doped with 20% of polypyrrole (CB-PPy) purchased from Sigma Aldrich with an electrical conductivity of 3×10^{1} S.cm^{-1} and a relative density of 2.22 g.cm^{-3}.

2.2 | Sample preparation

2.2.1 | Preparation of CB-PPy composites

The composites were produced by melt compounding using a Thermo-Haake Polylab Rheomix 600 internal mixer with 50 cm^3 of internal volume and counter-rotating rotors. Composites based on the neat polymers PVDF and TPU and on PVDF/TPU blends with two different compositions comprising various amount of CB-PPy were prepared according to the formulations displayed in Table 1. The composition of the PVDF/TPU blends was selected based on preliminary work[33] due to the high flexibility achieved in the 38/62 vol% blend and the formation of a co-continuous structure in the 50/50 vol % blend. Various fractions of the carbonaceous filler were added to the selected matrices to investigate the effect of filler content on the final materials' properties.

Before mixing, the materials were dried overnight at 60°C. Then, predetermined amounts of PVDF and/or TPU were added to the mixing chamber at 180°C at a rotor speed of 50 rpm. After 2 min, the conductive filler CB-PPy was introduced and left to mix for 13 more minutes.

2.2.2 | Compression molding

The composites with formulation displayed in Table 1 were then compression molded in squares plaques of 120 × 120 × 2 mm^3 using a Carver Laboratory press at 180°C applying a pressure of 3.9 MPa for 10 min. Compression-molded samples were cut in specific formats for various tests. In addition, samples for the EMI-SE analysis were compression molded in square plaques of 45 × 45 × 2 mm^3 by a BOVENAU P15 ST hydraulic press under the same conditions.

2.2.3 | Fused filament fabrication

According to our previous works,[33,34] PVDF/TPU/CB-PPy 38/62 vol % with 5% and 6% of CB-PPy and PVDF/TPU/CB-PPy 50/50 vol% with 10% of CB-PPy were selected for the preparation of extruded filaments to be used as feeding material in the fused filament fabrication (FFF). For the filament extrusion, the melt compounded composites were immersed in liquid nitrogen and then grinded. The obtained powder was used to feed a single screw extruder Friul Filiere SpA model Estru 13 at 30 rpm with four temperature zones of 130, 170, 175, and 180°C (die), and filaments with 1.75 ± 0.10 mm of diameter were fabricated. The filaments were printed by a Sethi S3 3D printer based on the fused filament fabrication technology. Square plaques of 45 × 45 × 2 mm were build-up along horizontal alternate (H45) direction with rectangular infill of 100%. The open source software Slic3r was used to slice the drawing in 10 layers of 0.2 mm each and to settle the following printing parameters: nozzle diameter 0.4 mm; nozzle

TABLE 1 Composition of prepared composites.

CB-PPy (%)			
PVDF/CB-PPy	TPU/CB-PPy	PVDF/TPU/CB-PPy 38/62 vol%	PVDF/TPU/CB-PPy 50/50 vol%
0	0	0	0
1	-	-	1
2	-	-	2
3	3	3	3
5	5	5	5
6	6	6	6
7	7	7	-
10	10	10	10
-	-	15	-

temperature 240°C; nozzle speed 40 mm.s^{-1} and printing platform temperature 70°C.

2.3 | Testing techniques

Rheology analysis was carried out in oscillatory mode by a Discovery DHR 1 rheometer from TA Instrument Inc. operating with parallel plates of 25 mm of diameter and 1.0 mm of gap for specimens with lower than 10% of conductive filler and 1.2 mm of gap for specimens with 10% or higher content of conductive filler. The measurements were performed at 180°C under nitrogen atmosphere with frequencies ranging from 0.1 to 100 Hz and a strain amplitude of 0.1%.

Dynamic mechanical thermal analysis (DMTA) was performed by a Netzsch DMA 242 E device under tensile mode from −80 to 100°C at a frequency of 1 Hz. The maximum dynamic strain applied was 50 μm and the heating heat was 3°C.min^{-1}. The measurements were performed on rectangular specimens of 20 × 5 × 2 mm^3 and the gauge length was 10 mm.

Electrical conductivity measurements of high conductive samples were carried out using an ASTM D4496-04 four-probe standard configuration using an ISO-TECH IPS303DD DC power supply as a voltage source and an ISO-TECH IDM 67pocket multimeter with a 3.69 mm internal electrode to measure the current flow. Both sides of three rectangular samples of 36.9 × 5 × 2 mm^3 were measured. For electrical conductivity measurements of high resistive samples a two-probe standard configuration was adopted by using a Keithley 6517A electrometer linked to a Keithley 8009 resistivity test fixture. Samples with 2 mm of thickness were tested on both sides.

Electromagnetic interference shielding effectiveness (EMI-SE) measurements were performed in the X-band frequency range (from 8.2 to 12.4 GHz) using an N5230C Agilent Technology PNA series analyzer connected to a rectangular waveguide of 23 × 10 mm^2 as a sample holder. The incident electromagnetic wave (I) was applied to the sample and the transmitted (T) and reflected (R) waves were collected. The total EMI-SE of electrically conductive polymer composites is composed of the shielding effectiveness by reflection (SE_R) and the shielding effectiveness by absorption (SE_A), which are described in the following equation:

$$SE_R = 10\log\frac{I}{I-R}; SE_A = 10\log\frac{I-R}{T}; \text{EMI} - SE = SE_R + SE_A = 10\log\frac{I}{T}$$

3 | RESULTS AND DISCUSSION

3.1 | Rheology measurements

The rheology measurements were performed in order to investigate structural changes related to the interaction between the components and to the formation of a tridimensional filler network in the polymeric matrices.[12,26,35] A comparison of the curves of storage modulus (G′) and complex viscosity (η*) as a function of frequency between the composites based on the neat polymers and on the polymer blends as matrices with 5% and 10% of CB-PPy are presented in Figure 1. The curves show that the composites composed of the PVDF/TPU blend as matrix present an intermediate behavior between those found for the composites based on the neat polymers. It is also noticeable that, as discussed before, the effect of filler is much more pronounced in PVDF. As the filler content is increased, the rheological behavior of PVDF/TPU/CB-PPy composites becomes more similar to the rheological behavior of neat PVDF/CB-PPy composites indicating that the filler restricts more efficiently the movement of the polymeric chains of PVDF leading to higher storage modulus and higher complex viscosity.

A summary of the main rheological properties for the PVDF/CB-PPy and TPU/CB-PPy composites are shown in Table 2 and for the PVDF/TPU/CB-PPy composites in Table 3. For all composites, the addition of CB-PPy generally increases the storage modulus (G′) and complex viscosity (η*) of the composites due to the formation of a tridimensional network by the filler leading to the reduction of the mobility of the polymeric chains. When comparing PVDF/CB-PPy and TPU/CB-PPy composites, the effect of filler is much more pronounced in PVDF composites. For instance, when 10% of CB-PPy is added to PVDF/CB-PPy composites, an increases of almost 346 times in G′ and 177 times in η* can be observed. On the other hand, when 10% of CB-PPy is added to TPU/CB-PPy composites, the increase in G′ and η* is about 4 and 2 times, respectively. It can be related to a poorer dispersion of CB-PPy in TPU or some degree of plasticizer effect when low concentrations of CB-PPy are added to the TPU matrix. Moreover, the addition of an elevated amount of filler (i.e. 10%) to PVDF/TPU/CB-PPy composites leads to a blunt drop in G′ and η* with increasing the frequency, which is related to a shear thinning behavior characteristic of the pseudo-plastics behavior.

Figure 2 presents a comparison between the storage modulus (G′) and loss modulus (G″) curves for composites comprising (A) 5% and (B) 10% of CB-PPy.

For PVDF-based composites with 5% and 10% of CB-PPy, G′ is higher than G″ for the whole frequency range indicating a solid-like behavior. Although G′ is slightly higher than G″ for PVDF/CB-PPy 5%, when 10% of filler is added to the composite, G′ is significantly higher than the G″ in the whole frequency range indicating there is the creation of a tridimensional network in higher degree leading to a material with more solid behavior. On the other hand, TPU/CB-PPy composites show storage modulus (G′) higher than loss modulus (G″) at low frequencies representing a solid-like behavior, however, at a specific frequency G′ and G″ curves are intercepted and G″ becomes higher than G′ demonstrating a liquid-like behavior. This behavior is less pronounced with increasing the CB-PPy content. For composites based on the PVDF/TPU blends, those with 5% of CB-PPy show an intermediate behavior between the composites based on the neat polymers with the same filler content. PVDF/TPU/CB-PPy 38/62 vol% reports a rheological behavior a bit more influenced by the TPU rheology than PVDF/TPU/CB-PPy 50/50 vol%, that presents G′ and G″ curves more

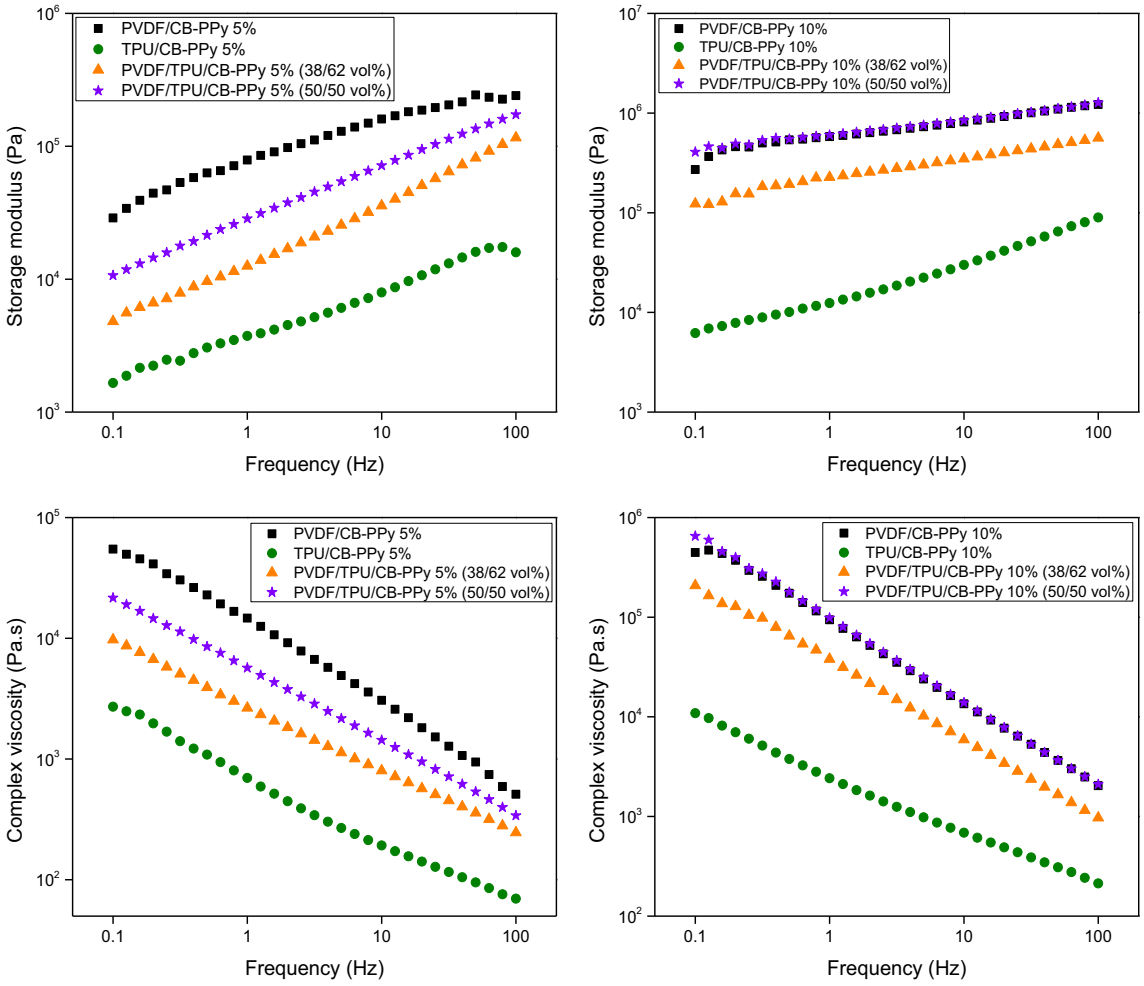

FIGURE 1 Storage modulus (G′) and complex viscosity (η*) as function of frequency for composites with 5% and 10% of CB-PPy.

TABLE 2 Summary of main rheological properties at 180°C of compression molded PVDF/CB-PPy and TPU/CB-PPy composites.

Sample	Viscosity at 10^{-1} Hz (Pa.s)	G′ at 10^{-1} Hz (Pa)	G″ at 10^{-1} Hz (Pa)
PVDF	533	1678	2896
PVDF/CB-PPy 3%	3360	13,703	16,058
PVDF/CB-PPy 5%	14,690	78,816	48,035
PVDF/CB-PPy 10%	94,265	579,944	120,271
Sample	**Viscosity at 10^{-1} Hz (Pa.s)**	**G′ at 10^{-1} Hz (Pa)**	**G″ at 10^{-1} Hz (Pa)**
TPU	1352	3122	7900
TPU/CB-PPy 3%	941	4953	3227
TPU/CB-PPy 5%	697	3743	2272
TPU/CB-PPy 10%	2421	12,409	8794

related to the PVDF/CB-PPy since the amount of PVDF is higher is this composite. However, when the filler content is increased to 10%, the influence of PVDF on the composites rheology is more evident. In fact, PVDF/TPU/CB-PPy 50/50 vol% and PVDF/CB-PPy with 10% of filler display overlapped curves in the whole frequency range and the PVDF/TPU/CB-PPy 38/62 vol% curves are more similar to PVDF/CB-PPy than to TPU/CB-PPy even if the content of TPU in the blend is higher than the PVDF content.

The phase angle of PVDF/CB-PPy and TPU/CB-PPy composites was investigated and compared to the values found for PVDF/TPU/CB-PPy 38/62 vol% and PVDF/TPU/CB-PPy 50/50 vol% composites. The phase angle curves for the mentioned compression molded composites comprising 10% of CB-PPy are displayed in Figure 3. Higher phase angles, as those found for TPU/CB-PPy 10%, indicate that the material flows viscously as a liquid. On the other hand, lower phase angles are related to

TABLE 3 Summary of main rheological properties at 180°C of compression molded PVDF/TPU/CB-PPy composites.

PVDF/TPU 38/62 vol%			
CB-PPy (%)	**Viscosity at 10^{-1} Hz (Pa.s)**	**G′ at 10^{-1} Hz (Pa)**	**G″ at 10^{-1} Hz (Pa)**
0	700[34]	2184[34]	3816[34]
3	1022[34]	4114[34]	4927[34]
5	2647[34]	12,556[34]	10,910[34]
6	4931[34]	25,979[34]	16,886[34]
10	37,962[34]	226,762[34]	73,971[34]
PVDF/TPU 50/50 vol%			
CB-PPy (%)	**Viscosity at 10^{-1} Hz (Pa.s)**	**G′ at 10^{-1} Hz (Pa)**	**G″ at 10^{-1} Hz (Pa)**
0	815	2421	4515
1	1357	4283	7372
3	1934	7431	9612
5	5694	28,557	21,556
10	98,279	601,647	139,059

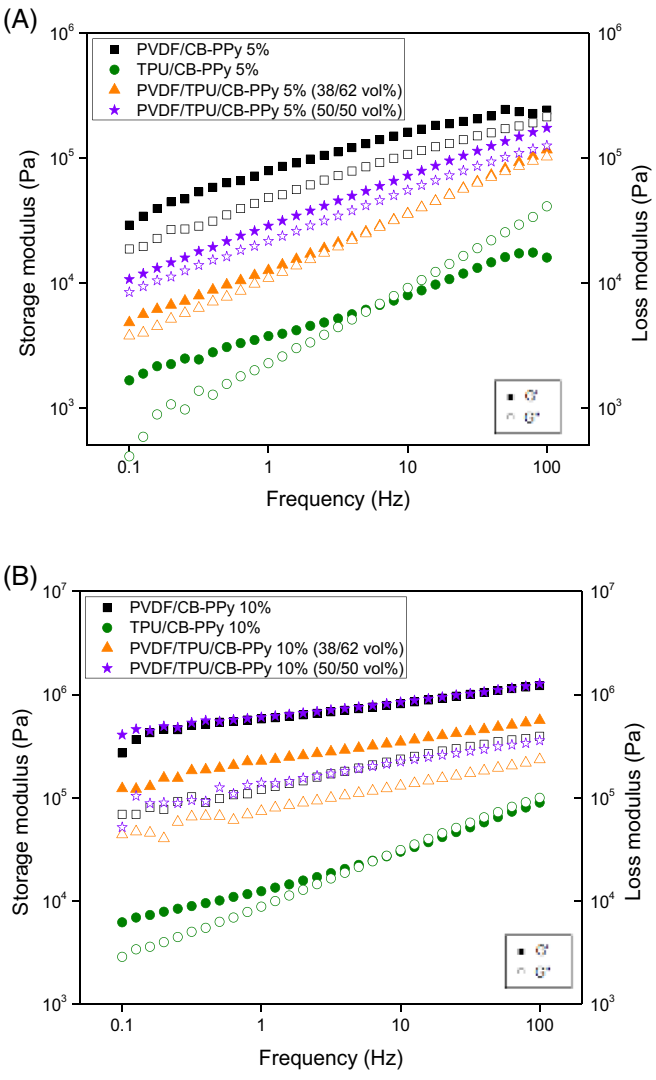

FIGURE 2 Storage and loss modulus as a function of frequency for composites with 5% and 10% of CB-PPy.

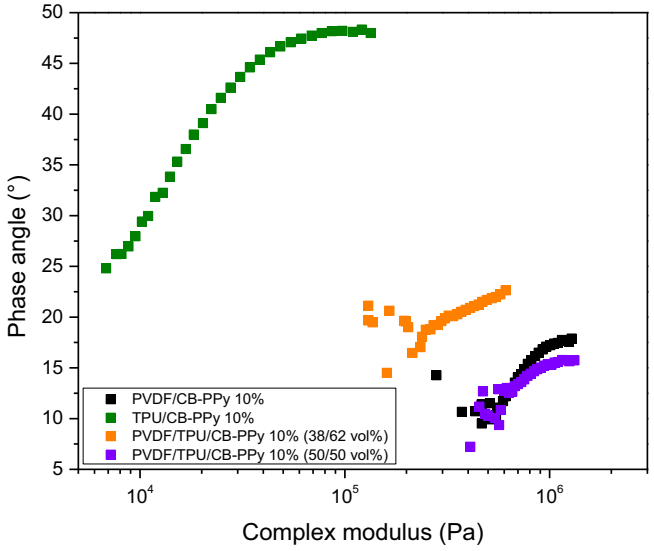

FIGURE 3 Phase angle as a function of complex modulus in the molten state for composites with 10% of CB-PPy.

materials that deform more elastically as a solid. Lower values of phase angle are found for PVDF/CB-PPy 10% and PVDF/TPU/CB-PPy 38/62 vol% and 50/50 vol% with 10% of CB-PPy. In addition, the phase angle values for the composites based on the PVDF/TPU blends are between those obtained for the composites based on the neat polymers as matrix. However, the PVDF/TPU/CB-PPy 50/50 vol% co-continuous composite presents a phase angle curve very similar to the curve of PVDF/CB-PPy, thus corroborating the idea that PVDF has a more significant effect on the rheological behavior of the composites. For as the format of the curves is concerned, a semi-circle format found for the phase angle curves indicates a good dispersion of the filler in the PVDF/TPU matrices.

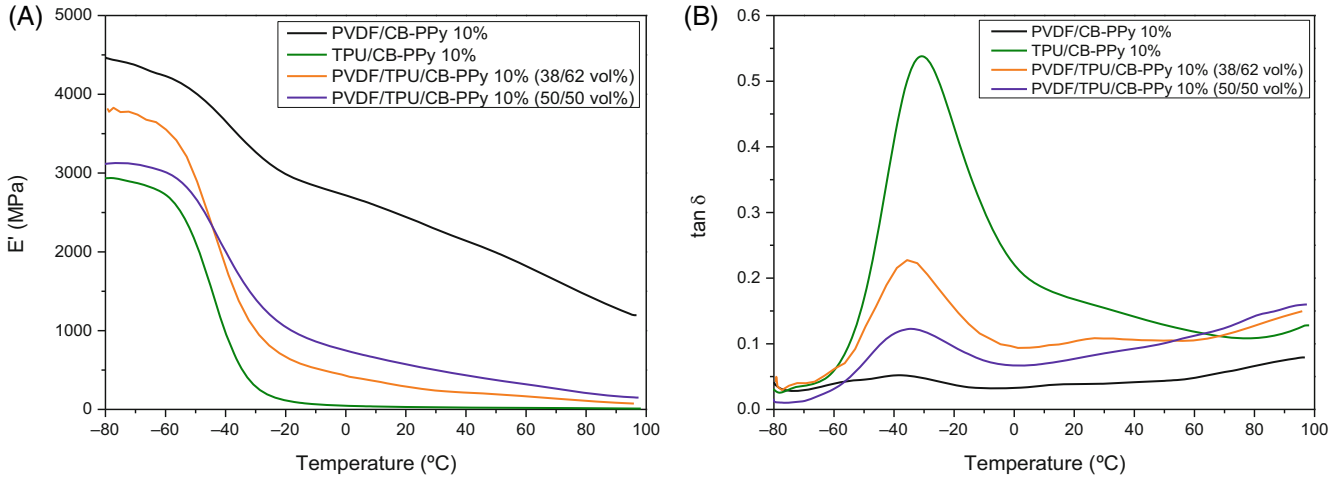

FIGURE 4 (A) Storage modulus (E′) and (B) loss tangent (tan δ) as a function of temperature for compression molded composites with 10% of CB-PPy.

TABLE 4 Glass transition temperature (T_g) for compression molded composites with 10% of CB-PPy.

Sample	T_g (°C)
PVDF/CB-PPy 10%	−39.1
PVDF/TPU/CB-PPy 10% (38/62 vol%)	−35.2[34]
PVDF/TPU/CB-PPy 10% (50/50 vol%)	−34.3
TPU/CB-PPy 10%	−30.8

3.2 | Dynamic mechanical thermal analysis (DMTA)

Figure 4 presents the variation of (a) E′ and (b) tan δ (loss tangent) with temperature for the composites comprising 10% of CB-PPy. Considering the composites comprising 10% of CB-PPy, the storage modulus curves show that the highest storage modulus corresponds to the sample composed of PVDF/CB-PPy, while the lowest storage modulus is attributed to the TPU/CB-PPy composite. The composites based on the PVDF/TPU blends display a storage modulus curve between those found for the composites based on the neat polymers indicating that the addition of TPU to the blends assists the production of composites with improved flexibility. The glass transition temperature (T_g) follows the same pattern where T_g of composites based on the neat polymers present the highest and lowest values (i.e. −39.1°C for PVDF/CB-PPy and −30.8°C for TPU/CB-PPy), while the T_g values for the composites based on the PVDF/TPU blends are between those found for PVDF/CB-PPy and TPU/CB-PPy. The glass transition temperature values measured from the tan δ peak are displayed Table 4. The influence of the conductive filler CB-PPy on the storage modulus and glass transition temperature of the composites was already discussed in our previous work.[34] Overall, increasing the content of CB-PPy was found to increase the storage modulus of the composites leading to more rigid materials and to decrease the T_g values of the composites.

3.3 | Electrical conductivity

The electrical conductivity of the compression molded composites comprising the different matrices and various amount of filler was measured and reported in Table 5. The electrical conductivity of all studied composites increases with the addition of CB-PPy. When comparing composites with same amount of filler, the PVDF-based composites present higher electrical conductivity than the TPU-based composites, while PVDF/TPU 38/62 vol% composites show an intermediate value of electrical conductivity. On the other hand, the composites based on the co-continuous blend of PVFD/TPU 50/50 vol% display a much higher electrical conductivity than the 38/62 vol % composites, indicating that the formation of a co-continuous structure can improve the electrical conductivity of the composites probably due to the selective localization of the filler in one phase or at the interface of the polymeric blend.[28]

Moreover, as already discussed in our previous papers,[33,34] the electrical conductivity of samples prepared by FFF is significantly lower when compare to compression molded composites with the same composition due to the presence of voids, defects and overlapping layers that can hinder the electrons flow.[3,6,36,37] In summary, after the 3D printing process, the only composite among those investigated that displayed a still high value of electrical conductivity was PVDF/TPU/CB-PPy with 10% of filler, which presented an electrical conductivity of 4.14×10^0 S.m^{-1}.

3.4 | Electromagnetic interference shielding effectiveness (EMI-SE)

The EMI-SE of the composites with various amount of CB-PPy was investigated in the X-band frequency range, from 8.2 to 12.4 GHz. The effect of the conductive filler and polymeric matrices was evaluated. The total SE, SE_R, and SE_A of PVDF/CB-PPy and TPU/CB-PPy compression molded composites are displayed in Figures 5 and 6,

TABLE 5 Electrical conductivity of compression molded composites with various amount of conductive filler.

Electrical conductivity σ (s.m^{-1})				
CB-PPy (%)	**PVDF/CB-PPy**	**TPU/CB-PPy**	**PVDF/TPU/CB-PPy 38/62 vol%**	**PVDF/TPU/CB-PPy 50/50 vol%**
0	$(5.73 \pm 0.76) \times 10^{-13}$	$(9.39 \pm 0.42) \times 10^{-11}$	$(1.60 \pm 0.03) \times 10^{-11}$[33]	$(1.99 \pm 0.10) \times 10^{-11}$
1	$(1.65 \pm 0.12) \times 10^{-9}$	-	-	$(1.42 \pm 0.43) \times 10^{-11}$
2	$(3.49 \pm 2.26) \times 10^{-1}$	-	-	$(5.30 \pm 2.85) \times 10^{-11}$
3	$(1.48 \pm 0.16) \times 10^{0}$	$(3.07 \pm 1.40) \times 10^{-9}$	$(3.19 \pm 0.03) \times 10^{-10}$[34]	$(4.49 \pm 4.27) \times 10^{-1}$
5	$(7.82 \pm 2.92) \times 10^{0}$	$(4.94 \pm 0.02) \times 10^{-9}$	$(7.95 \pm 4.82) \times 10^{-7}$[33]	$(1.18 \pm 0.29) \times 10^{0}$
6	$(1.82 \pm 0.03) \times 10^{1}$	$(4.21 \pm 2.74) \times 10^{-8}$	$(1.94 \pm 1.04) \times 10^{-1}$[33]	$(1.69 \pm 0.26) \times 10^{0}$
7	$(4.81 \pm 0.26) \times 10^{1}$	$(4.35 \pm 3.96) \times 10^{-2}$	$(6.44 \pm 0.64) \times 10^{-1}$[34]	-
10	$(6.16 \pm 0.49) \times 10^{1}$	$(2.77 \pm 0.02) \times 10^{0}$	$(5.90 \pm 0.52) \times 10^{0}$[34]	$(1.70 \pm 0.24) \times 10^{1}$[33]
15	-	-	$(3.23 \pm 0.17) \times 10^{1}$[34]	-

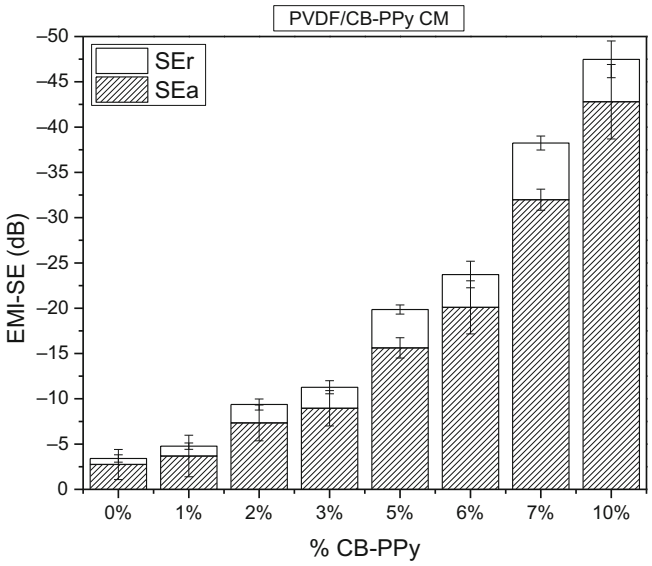

FIGURE 5 Total SE, SE_R, and SE_A as a function of CB-PPy fraction for PVDF/CB-PPy composites prepared by compression molding.

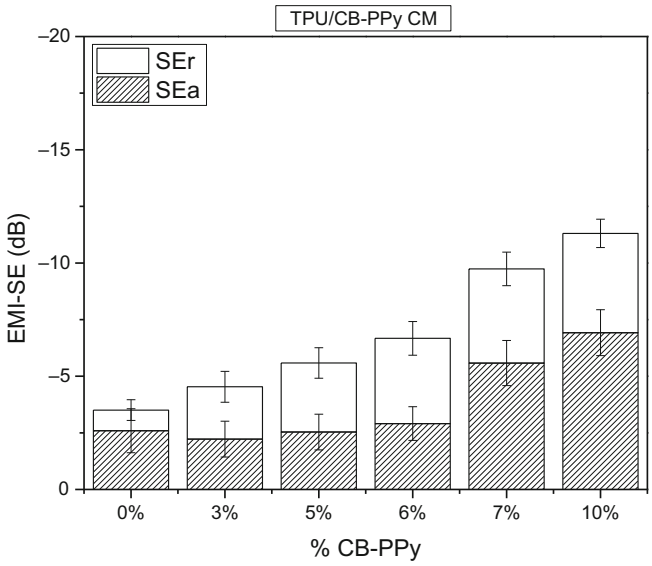

FIGURE 6 Total SE, SE_R, and SE_A as a function of CB-PPy fraction for TPU/CB-PPy composites prepared by compression molding.

respectively. In addition, the EMI-SE for the compression molded composites based on the PVDF/TPU blends are displayed in Figures 7 and 8. For all analyzed composites, the attenuation of the incident electromagnetic radiation is increased with the addition of CB-PPy. The results are in agreement with the electrical conductivity values found for those composites since according to other studies reported in the literature[3,11] the EMI-SE of electrically conductive polymer composites is expected to be enhanced as the electrical conductivity of the composites increases.

Moreover, the composites based on the PVDF/TPU blends exhibit EMI-SE values between those found for the composites based on the neat polymers. It is important to notice that the co-continuous composites, PVDF/TPU/CB-PPy 50/50 vol%, show a better compromise between electrical conductivity, mechanical properties, and EMI shielding efficiency since they are capable of reaching higher electromagnetic shielding values with lower amount of CB-PPy when compared to PVDF/TPU/CB-PPy 38/62 vol% composites. The less amount of conductive filler is added, the more preserved the mechanical properties and processability of the polymeric matrix will be.

Furthermore, most applications of electromagnetic shielding materials require a minimum attenuation of the electromagnetic waves of −20 dB, which corresponds to the shielding of more than 99% of the incident radiation.[5,11] This value was reached for compression molded composites of PVDF/CB-PPy with 5% of filler, however, for TPU/CB-PPy composites the minimum shielding value required for EMI shielding applications was not achieved at any filler content tested. For PVDF/TPU/CB-PPy 38/62 vol% compression molded composites, 15% of CB-PPy was necessary to reach the attenuation of at least −20 dB, while for the co-continuous PVDF/TPU/CB-PPy 50/50 vol% composites 10% is already enough.

In addition, the developed PVDF/TPU/CB-PPy show the advantages of higher contribution of the absorption mechanism that

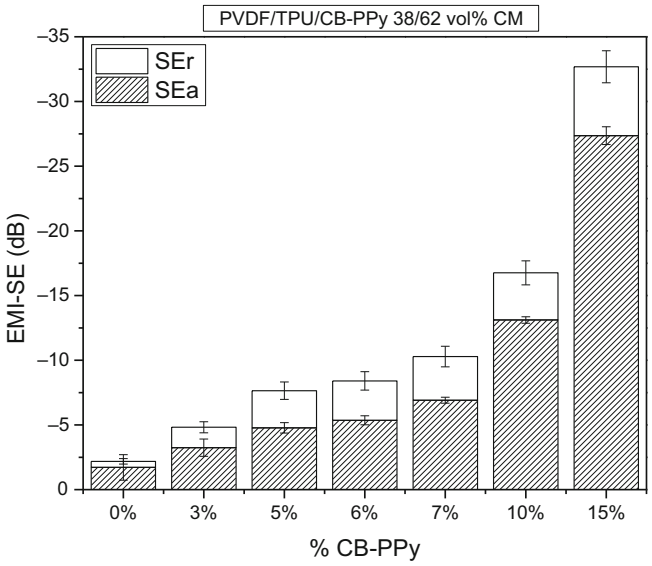

FIGURE 7 Total SE, SE_R, and SE_A as a function of CB-PPy fraction for PVDF/TPU/CB-PPy 38/62 vol% composites prepared by compression molding.

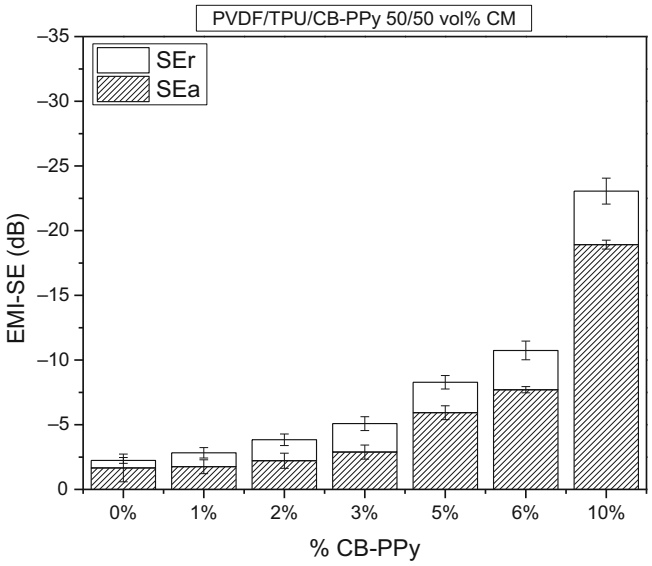

FIGURE 8 Total SE, SE_R, and SE_A as a function of CB-PPy fraction for PVDF/TPU/CB-PPy 50/50 vol% composites prepared by compression molding.

eliminates the electromagnetic waves, while the reflection may be a source of secondary pollution.

Another parameter that is evaluated in EMI shielding applications is the shielding effectiveness by absorption (SE_A) and the shielding effectiveness by reflection (SE_R). The particles of CB-PPy added to the composites interact with the electromagnetic waves absorbing (A) or reflecting (R) the electromagnetic radiation. The radiation that is not absorbed or reflected by the shielding material will be transmitted (T) to the environment. The stack plots reported in the above pictures show that the EMI-SE of all compression molded composites is the

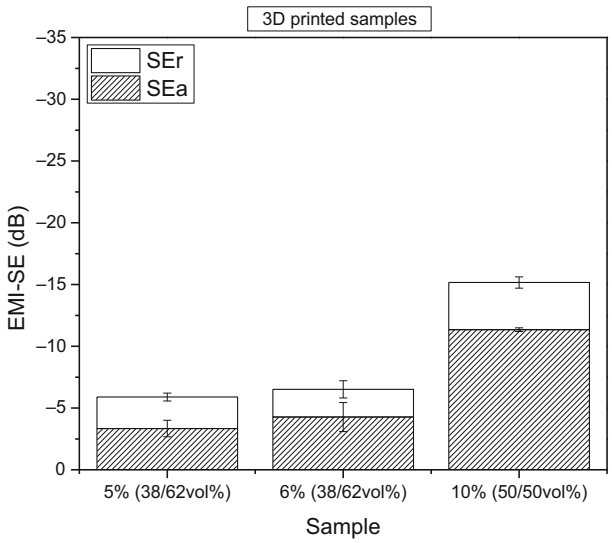

FIGURE 9 Total SE, SE_R, and SE_A as a function of CB-PPy fraction for PVDF/TPU/CB-PPy composites prepared by fused filament fabrication.

TABLE 6 Comparison of total EMI-SE values between compression molded (CM) and 3D printed (3D) composites.

	EMI-SE (dB)	
PVDF/TPU/CB-PPy	CM	3D
5% (38/62 vol%)	−7.6	−5.9
6% (38/62 vol%)	−8.4	−6.5
10% (50/50 vol%)	−23.0	−15.2

sum of reflection and absorption mechanisms and both are increased with the addition of CB-PPy. Nevertheless, the contribution of the absorption mechanism is generally higher for the investigated composites, which is required for some applications, for example in applications for military radars, since the absorption mechanism eliminates the electromagnetic radiation while the reflection may be a source of secondary pollution. For carbon-based composites, the commanding EMI shielding mechanism is commonly absorbed due to the composite's electrical properties.[5] However, for TPU/CB-PPy composites, the shielding of the incident electromagnetic radiation was found to be similar by absorption and reflection mechanisms.

Overall, PVDF/CB-PPy composites present much higher values of EMI-SE than TPU/CB-PPy composites, however, their mechanical flexibility is much lower. On the other hand, PVDF/TPU/CB-PPy 50/50 vol% co-continuous composites display a good balance between mechanical properties (as discussed in our previous works[33,34]) and EMI-SE values and are capable to reach −23 dB of EMI attenuation with 10% of filler, which is higher than the minimum value of attenuation required for shielding applications.

In addition, the 3D printed PVDF/TPU/CB-PPy composites were also investigated in order to evaluate the influence of the printing process on the EMI shielding effectiveness, and their stack plots with the

total EMI-SE, SE_R, and SE_A are presented in Figure 9. The total EMI-SE values of compression molded and 3D printed composites with the same composition are compared in Table 6. The results show that the samples prepared by fused filament fabrication have EMI-SE values lower than compression-molded samples with the same composition. For instance, the compression molded PVDF/TPU/CB-PPy 50/50 vol% composite with 10% of CB-PPy displays an EMI-SE of −23 dB, while the 3D printed composite with the same composition presents an EMI-SE of around −15 dB. The EMI-SE values are related to the volume conductivity of the samples. In fact, the 3D printed specimens presented a substantial drop in the electrical conductivity[33,34] when compared to the compression molded samples due to the presence of defects and voids in the 3D printed specimens occasioned by the layer-by-layer deposition, which is much lower in more compacted compression molded composites. In addition, the porous structure of 3D printed specimens results in a lower amount of material available to interact with the incident electromagnetic waves.

4 | CONCLUSIONS

In this study, the electromagnetic interference shielding effectiveness of composites based on immiscible polymer blends of PVDF/TPU filled with CB-PPy as conductive filler and based on neat PVDF and TPU filled with CB-PPy prepared by compression molded and fused filament fabrication was investigated.

The results show that the rheological behavior of the composites based on the PVDF/TPU blends as matrix presented a behavior intermediate between those found for the composites based on the neat polymers. In addition, the effect of filler was found to be much more pronounced in PVDF than in TPU. The storage modulus and glass transition temperature (T_g) of the composites follow the same pattern where the storage modulus curves and T_g values of PVDF/TPU/CB-PPy composites are between those found for the composites based on the neat polymers indicating that the addition of TPU to the blends assists the preparation of composites with improved flexibility. Moreover, as the content of CB-PPy increased, the storage modulus of the composites also increased leading to more rigid materials. Concurrently, the T_g values of the composites decreased.

The EMI-SE of the investigated composites resulted to be directly related to their electrical conductivity, i.e. to the content of the conductive filler CB-PPy. In fact, specimens with higher electrical conductivity reported higher shielding of the electromagnetic radiation since the amount of conductive particles that can interact with the electromagnetic radiation is higher. Furthermore, the main shielding mechanism of the investigated composites was found to be the absorption, which is desired for some technological applications.

Moreover, the composites based on the PVDF/TPU 50/50 vol% co-continuous blend as matrix displayed a better combination of EMI shielding efficiency and mechanical properties. For instance, the addition of 15% of CB-PPy was necessary to reach the attenuation of at least −20 dB (which corresponds to a shielding efficiency of more than 99% of the incident wave) in PVDF/TPU/CB-PPy 38/62 vol% composites, while the addition of 10% of CB-PPy was capable to induce the same level of EMI shielding in PVDF/TPU/CB-PPy 50/50 vol% co-continuous composites. Furthermore, specimens prepared by fused filament fabrication presented diminished values of electrical conductivity and EMI-SE response when compared to compression molded samples with the same composition due to the presence of voids and defects in the 3D printed parts.

ACKNOWLEDGMENTS

This research has been funded by the Italian Ministry for Education, University of Trento, and the Italian Ministry for University and Research (MUR) through the "Departments of Excellence" program and Mayara Cristina Bertolini is supported by the "Departments of Excellence" grant L.232/2016. This work was also supported by CNPq (Conselho Nacional de Desenvolvimento Científico e Tecnológico) grant 309125/2020-0 and CAPES-PRINT number 88881.310728/2018-01. The authors thank to the Instituto de Macromoléculas (IMA) at the Universidade Federal do Rio de Janeiro for the EMI-SE analysis and the rheology measurements.

DATA AVAILABILITY STATEMENT

The data that support the findings of this study are available from the corresponding author upon reasonable request.

ORCID

Mayara C. Bertolini https://orcid.org/0000-0003-2852-5450

REFERENCES

1. Viskadourakis Z, Vasilopoulos KC, Economou EN, Soukoulis CM, Kenanakis G. Electromagnetic shielding effectiveness of 3D printed polymer composites. *Applied Physics A*. 2017;123(12):1-7.
2. Thomassin J-M, Jérôme C, Pardoen T, Bailly C, Huynen I, Detrembleur C. Polymer/carbon based composites as electromagnetic interference (EMI) shielding materials. *Mater Sci Eng R Rep*. 2013;74(7):211-232.
3. Ecco L, Dul S, Schmitz D, et al. Rapid prototyping of efficient electromagnetic interference shielding polymer composites via fused deposition modeling. *Appl Sci*. 2018;9(1):37.
4. Mao Y-J, Xu L, Lin H, et al. Effective electromagnetic interference shielding properties of micro-truss structured CNT/epoxy composites fabricated based on visible light processing. *Compos Sci Technol*. 2022;221:109296.
5. Schmitz DP, Ecco LG, Dul S, et al. Electromagnetic interference shielding effectiveness of ABS carbon-based composites manufactured via fused deposition modelling. *Mater Today Commun*. 2018;15:70-80.
6. Dul S, Ecco LG, Pegoretti A, Fambri L. Graphene/carbon nanotube hybrid nanocomposites: effect of compression molding and fused filament fabrication on properties. *Polymers (Basel)*. 2020;12(1):101.
7. Omana L, Chandran A, John RE, et al. Recent advances in polymer nanocomposites for electromagnetic interference shielding: a review. *ACS Omega*. 2022;7(30):25921-25947.
8. Sit S, Nath K, das NC, Chakraborty G. Superior electromagnetic interference shielding effectiveness of functionalized MWCNTs filled flexible thermoplastic polymer nanocomposites. *J Elastomers Plast*. 2022;54(6):975-999.

9. Lee JH, Kim YS, Ru HJ, Lee SY, Park SJ. Highly flexible fabrics/epoxy composites with hybrid carbon Nanofillers for absorption-dominated electromagnetic interference shielding. *Nano Lett*. 2022;14(1):188.
10. Anand S, Muniyappan S, Racik KM, et al. Fabrication of binary to quaternary PVDF based flexible composite films and ultrathin sandwich structured quaternary PVDF/CB/g-C3N4/BaFe11.5Al0.5O19 composite films for efficient EMI shielding performance. *Synth Met*. 2022;291:117199.
11. Al-Saleh MH, Sundararaj U. A review of vapor grown carbon nanofiber/polymer conductive composites. *Carbon*. 2009;47(1):2-22.
12. Soares BG, Calheiros LF, Silva AA, Indrusiak T, Barra GM, Livi S. Conducting melt blending of polystyrene and EVA copolymer with carbon nanotube assisted by phosphonium-based ionic liquid. *J Appl Polym Sci*. 2018;135(24):45564.
13. Zhang H-Y, Li JY, Pan Y, Liu YF, Mahmood N, Jian X. Flexible carbon fiber-based composites for electromagnetic interference shielding. *Rare Metals*. 2022;41(11):3612-3629.
14. Paddubskaya A, Valynets N, Kuzhir P, et al. Electromagnetic and thermal properties of three-dimensional printed multilayered nano-carbon_poly(lactic) acid structures. *J Appl Phys*. 2016;119:135102.
15. Abedi K, Miri S, Gregorash L, Fayazbakhsh K. Evaluation of electromagnetic shielding properties of high-performance continuous carbon fiber composites fabricated by robotic 3D printing. *Addit Manuf*. 2022;54:102733.
16. Wang J, Li H, Wang Z, et al. Improved electromagnetic interference shielding properties of poly(vinylidene fluoride) composites based on carbon nanotubes and graphene nanoplatelets. *Polym Compos*. 2022;43(10):6966-6974.
17. Bleija M, Platnieks O, Macutkevič J, Starkova O, Gaidukovs S. Comparison of carbon-nanoparticle-filled poly(butylene succinate-co-Adipate) nanocomposites for electromagnetic applications. *Nanomaterials (Basel)*. 2022;12(20):3671.
18. Ramoa SDAS, Barra GMO, Merlini C, Livi S, Soares BG, Pegoretti A. Electromagnetic interference shielding effectiveness and microwave absorption properties of thermoplastic polyurethane/montmorillonite-polypyrrole nanocomposites. *Polym Adv Technol*. 2018;29(5):1377-1384.
19. Wang Y, Fan ZW, Zhang H, et al. 3D-printing of segregated carbon nanotube/polylactic acid composite with enhanced electromagnetic interference shielding and mechanical performance. *Mater Des*. 2021;197:109222.
20. Schmitz DP, Dul S, Ramoa SDAS, Soares BG, Barra GMO, Pegoretti A. Effect of printing parameters on the electromagnetic shielding efficiency of ABS/carbonaceous-filler composites manufactured via filament fused fabrication. *J Manuf Process*. 2021;65:12-19.
21. Rosa BDS, Merlini C, Livi S, Barra GMDO. Development of poly (butylene adipate-co-terephthalate) filled with montmorillonite-Polypyrrole for pressure sensor applications. *Mater Res*. 2019;22(2).
22. Menon AV, Madras G, Bose S. Magnetic alloy-MWNT Heterostructure as efficient electromagnetic wave suppressors in soft nanocomposites. *ChemistrySelect*. 2017;2(26):7831-7844.
23. Chatham CA, Zawaski CE, Bobbitt DC, Moore RB, Long TE, Williams CB. Semi-crystalline polymer blends for material extrusion additive manufacturing printability: a case study with poly(ethylene terephthalate) and polypropylene. *Macromol Mater Eng*. 2019;304(5):1800764.
24. Al-Saleh MH, Sundararaj U. An innovative method to reduce percolation threshold of carbon black filled immiscible polymer blends. *Compos A Appl Sci Manuf*. 2008;39(2):284-293.
25. Liu Y, Yang X, Yue L, Li W, Gan W, Chen K. Selective dispersion of silver nanowires in epoxy/polyetherimide binary composites with enhanced electrical conductivity: a study of curing kinetics and morphology. *Polym Compos*. 2019;40(11):4390-4401.
26. Lopes Pereira EC, Soares BG, Silva AA, Farias da Silva JM, Barra GMO, Livi S. Conductive heterogeneous blend composites of PP/PA12 filled with ionic liquids treated-CNT. *Polym Test*. 2019;74:187-195.
27. Shi YY, Yang JH, Huang T, Zhang N, Chen C, Wang Y. Selective localization of carbon nanotubes at the interface of poly(L-lactide)/ethylene-co-vinyl acetate resulting in lowered electrical resistivity. *Compos Part B Eng*. 2013;55:463-469.
28. Bizhani H, Nayyeri V, Katbab AA, Jalali-Arani A, Nazockdast H. Double percolated MWCNTs loaded PC/SAN nanocomposites as an absorbing electromagnetic shield. *Eur Polym J*. 2018;100:209-218.
29. Chen J, Cui X, Zhu Y, Jiang W, Sui K. Design of superior conductive polymer composite with precisely controlling carbon nanotubes at the interface of a co-continuous polymer blend via a balance of π-π interactions and dipole-dipole interactions. *Carbon*. 2017;114:441-448.
30. Bera M, Saha U, Bhardwaj A, Maji PK. Reduced graphene oxide (RGO)-induced compatibilization and reinforcement of poly(vinylidene fluoride) (PVDF)–thermoplastic polyurethane (TPU) binary polymer blend. *Applied Polymers*. 2019;136(5):47010.
31. Nath K, Ghosh S, Ghosh SK, Das P, Das NC. Facile preparation of light-weight biodegradable and electrically conductive polymer based nanocomposites for superior electromagnetic interference shielding effectiveness. *J Appl Polym Sci*. 2021;138(22):50514.
32. Zhang H, Heng Z, Zhou J, et al. In-situ co-continuous conductive network induced by carbon nanotubes in epoxy composites with enhanced electromagnetic interference shielding performance. *Chem Eng J*. 2020;398:125559.
33. Bertolini MC, Dul S, Barra GMO, Pegoretti A. Poly(vinylidene fluoride)/thermoplastic polyurethane flexible and 3D printable conductive composites. *J Appl Polym Sci*. 2020;138(17):50305.
34. Bertolini MC, Dul S, Lopes Pereira EC, Soares BG, Barra GMO, Pegoretti A. Fabrication and characterization of piezoresistive flexible pressure sensors based on poly(vinylidene fluoride)/thermoplastic polyurethane filled with carbon black-polypyrrole. *Polym Compos*. 2021;42:6621-6634.
35. Lopes Pereira EC, da Silva MECF, Pontes K, Soares BG. Influence of protonic ionic liquid on the dispersion of carbon nanotube in PLA/-EVA blends and blend Compatibilization. *Front Mater*. 2019;6:234.
36. Dorigato A, Moretti V, Dul S, Unterberger SH, Pegoretti A. Electrically conductive nanocomposites for fused deposition modelling. *Synth Met*. 2017;226:7-14.
37. Gutierrez BJA, Dul S, Pegoretti A, Alvarez-Quintana J, Fambri L. Investigation of the effects of Multi-Wall and Single-Wall carbon nanotubes concentration on the properties of ABS nanocomposites. *C*. 2021;7(2):33.

How to cite this article: Bertolini MC, Ramoa SDAS, Pereira ECL, Soares BG, Barra GMO, Pegoretti A. Poly (vinylidene fluoride) and thermoplastic polyurethane composites filled with carbon black-polypyrrole for electromagnetic shielding applications. *Polym Adv Technol*. 2023;34(12):3838-3848. doi:10.1002/pat.6184